KADUNA JOURNAL OF GEOGRAPHY
2026, VOL. 8, No. 1, 321-330
https://doi.org/10.47514/kjg.2026.08.01.034

Research Article

Spatiotemporal Impact of Artisanal and Small-Scale Mining Activity on Land Use/Land Cover Dynamics in Du, Jos South, Nigeria

Emmanuel Niagma Tsenkus [a], Haruna D. Musa [a]

[a] Department of Urban and Regional Planning, Federal University of Technology, Minna, Nigeria.

ABSTRACT

Artisanal and small-scale mining (ASM) is a primary driver of spatiotemporal land use/land cover (LULC) change in Sub-Saharan Africa, yet longitudinal multi-temporal mapping at the community scale remains limited. This study quantifies 15-year (2010–2025) LULC dynamics and the spatial distribution of ASM activities in Du Area, Jos South, Plateau State, using Landsat 7 ETM (2010 at 30 m) and Sentinel-2 MSI (2015, 2020, and 2025 at 10 m) imagery. A random forest supervised classifier in the Semi-Automatic Classification Plugin (SCP) v8.5.0 was used with eight classes: water bodies, abandoned mining pits, natural vegetation, irrigated cropland, bare cropland, built-up areas, and bare soil, while the nearest neighbour analysis was used to determine the spatial distribution. The MOLUSCE plugin was used to generate a complete 8×8 transition matrix across all 64 class land cover classes, including active ASM. Results reveal that active ASM expanded 348.01% from 107.76 ha (2010) to 482.76 ha (2025), with the most significant growth between 2015 and 2020 (+300.84 ha, +220.7%). Irrigated cropland declined 62.7% (326.24 ha), the built-up area contracted 28.2% (545.40 ha), bare soil was depleted 84.3% (396.72 ha), and 86.20 ha of water-filled legacy pits persist as an unclaimed public health hazard. NNA confirmed strong and consistent ASM clustering across all four periods (2025: NNI = 0.6519, z = −34.20, p < 0.001; observed mean inter-site distance 72.22 m). The study reveals that Du is undergoing intensifying spatial environmental degradation driven by unregulated ASM expansion.

ARTICLE HISTORY
Submitted 11 March 2026
Accepted 12 May 2026
Published 21 May 2026

GUEST EDITOR
A. M. Ahmed

KEYWORDS
Land use/land cover change, artisanal and small-scale mining, random forest classification, Nearest neighbour analysis, spatiotemporal analysis

1 Introduction

Land use and land cover (LULC) change is one of the most critical drivers of environmental transformation globally, particularly in developing countries where rapid population growth, agricultural expansion, and unregulated resource extraction are altering landscapes at unprecedented rates (Merem et al., 2017). Artisanal and Small-Scale Mining (ASM) remains a crucial driver of increased pressure on land resources due to its economic significance, especially in many developing countries, as it provides income to millions of individuals and is categorised among the most important non-farm rural income activities in Africa. ASM has expanded considerably due to the rise in mineral demand, widespread unemployment, and limited livelihood alternatives. Despite its significance, ASM ranges from informal individual miners earning a subsistence livelihood to more formal and regulated small-scale entities producing minerals commercially. The sector is characterised by low capital investment and labour-intensive operations, which contribute to both positive economic outcomes and severe environmental and social challenges.

This transition from formal to informal mining has deeply affected land use patterns and human safety, particularly in Du, Jos South LGA. Du has evolved into a hotspot of mining; the inflow of unregulated miners has led to a large number of degraded sites with abandoned mine pits, vegetation loss, and exposure to pollutants linked to surface and groundwater contamination, causing health risks to local populations (Gospel et al., 2020; Mafuyai et al., 2020, Ndace & Danladi, 2012). In addition, the geographic and environmental characteristics of the Jos Plateau, comprising porous soils, hilly terrains, and rainfall variability, further intensify the environmental footprint of these activities (NiMet, 2023).

Despite the critical impacts of ASM-related environmental challenges, spatially explicit multi-temporal LULC assessments at the community scale remain scarce. Existing research focused on either single-date mapping (Kumi-Boateng & Stemn, 2020) or large-scale levels of assessments of mining impact, paying little attention to community-based levels of vulnerabilities, environmental exposure, and risk. Kumi-Boateng and Stemn (2020) conduct a single-date mapping exercise; Couttenier et al. (2022) note the temporal potential of their approach but did not apply it to long-term degradation trajectories. While Kumi-Boateng and Stemn (2020) and Couttenier et al. (2022) used the Area of Interest proximity framework to demonstrate detection within distance buffers around large-scale mines, it fails to quantify the statistical correlation between distance and ASM sites. Many assessments focus on pollution metrics or economic outputs, overlooking the community-based spatial assessment of mining impacts (Muromba & Xu, 2024).

Corresponding Author: Tsenkus, E. N. emmanuel.tsenkus@st.futminna.edu.ng Department of Urban and Regional Planning, FUT Minna, Nigeria.
© 2026 The Author(s)

Various Land Use Land Cover (LULC) studies lacked the use of the Land Use Transition Metric (LUTM) to establish the class-to-class land use change due to the mining activities. This method is relevant in understanding the magnitude and direction of change, especially in locations with informal mining changing uses from residential, agricultural, or environmental spaces (Muromba & Xu, 2024). While other research studies have clearly mapped out trends of impact that focused on the physical and environmental degradation of mining-related activities, these studies failed to map and analyse the hotspot of mining-related incidents.

This study, therefore, addresses this gap by providing a 15-year multi-temporal LULC analysis and ASM spatial distribution assessment to assess environmental footprint changes in the Du Area. This study addresses a knowledge gap by providing the first 15-year multi-temporal LULC analysis (2010–2025) and ASM spatial distribution assessment for Du, Jos South, a region with historical tin mining legacy on the Jos Plateau. By quantifying spatiotemporal environmental changes across active and abandoned mining sites, this research provides evidence of environmental transformation rates important for informing reclamation policies. The findings directly address Nigeria's National Mining Cadastre requirement for environmental impact assessment and contribute baseline data for sustainable mining governance frameworks on the Jos Plateau. Furthermore, this localized assessment offers a replicable methodology to similar mining regions across sub-Saharan African nations.

2 Materials and Methods

2.1 Study Area

The Du community is located in the Jos South Local Government Area, Plateau State, north-central Nigeria. It is located between Latitudes 9°44′ and 9°48′N, Longitudes 8°50′ and 8°54′E (Figure 1). The region features a plateau at 1,200–1,800m above sea level underlain by a younger granite complex rich in tin, columbite, and lithium (Bala et al., 2021).

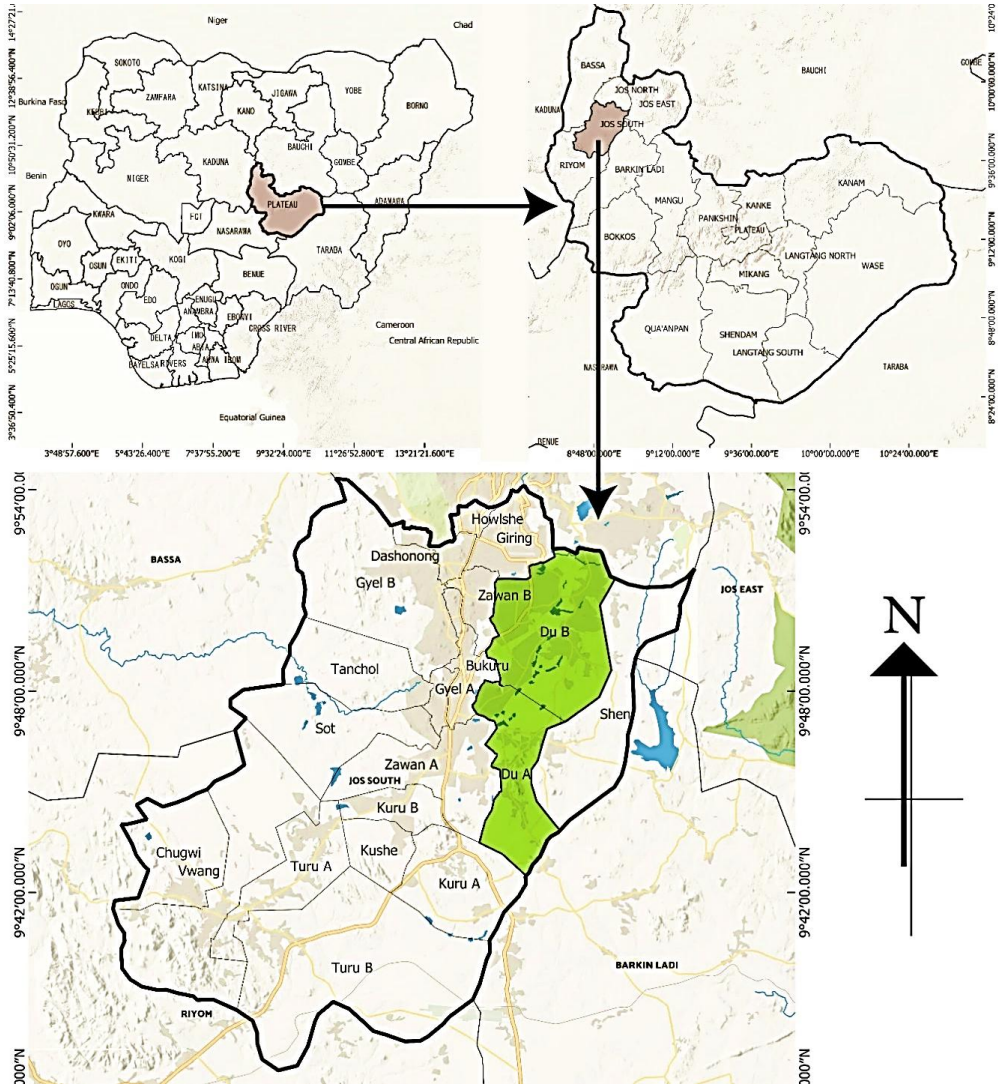

Figure 1: Study Area (Student Research Work, 2025)

The study area covers 7,420.60 ha. The soil is largely ferruginous tropical soil developed from granite and basaltic parent rock, generally sandy to sandy-loam in texture, well-drained, and moderately fertile under natural vegetation cover. However, their shallow depth and low organic matter content make them highly vulnerable to erosion, particularly when vegetation is removed (Adeyemi & Olagunju, 2015). Subsistence agriculture, informal mining, and scattered settlement characterise the dominant land-use pattern. The region experiences a sub-humid tropical highland climate characterised by two distinct seasons: the wet season (April–October) and the dry season (November–March). Du Ward has an estimated population of 45,604 (NPC, 2024), increasingly dependent on ASM following the collapse of formal mining in the 1980s.

2.2 Data Sources

LULC data were derived from Landsat 7 ETM imagery (30 m resolution) for 2010 using the USGS Earth Explorer platform. Sentinel-2 MSI imagery (10 m resolution) was acquired from the ESA Copernicus Open Access Hub for 2015, 2020, and 2025. All imagery was acquired during dry-season windows (January–February, cloud cover ≤10%) to minimise seasonal vegetation variation effects on classification accuracy (Couttenier et al., 2022; Nava et al., 2022).

2.3 Image Processing Classification

Preprocessing was conducted on the satellite imagery to rectify the scan-line error and atmospheric correction using QGIS. Layer stacking normalised band sets and wavelengths. The study area was extracted using administrative boundary shapefiles. Training samples were digitised from band composite and visual interpretation of ASM activity signatures supplemented by Google Earth visual interpretation for 2010, 2015, 2020 and 2025, creating a comprehensive Training Signature Files/ROI Database. A random forest supervised classification algorithm was applied within SCP v8.5.0 using eight classes and NNA module of the spatial analysis tool in Quantum Geographic Information System (QGIS) were employed (Congedo, 2021). Eight LULC classes were defined and adapted for ASM contexts (Table 1): Active ASM, Mining Water Bodies, Abandoned Mining Pits, Natural Vegetation, Irrigated Cropland, Bare Cropland, Built-up, and Bare Soil. Training samples were developed from 86 GPS field-verified ground-truth points collected across 23 localities in 2025.

Table 1: LULC Classification Scheme and Training Samples

MC_ID	MC_Name	Class Name	Category
1	Active Artisanal and Small-Scale Mining	ASM	Mining Impact – Active
2	Mining Water Bodies	Active Pits	Mining Impact – Active
3	Abandoned Mining Pits	Water filled	Mining Impact – Legacy
4	Natural Vegetation	Trees and Shrubs	Baseline – Vegetation
5	Irrigated Cropland	Irrigated Agriculture Land	Agriculture
6	Bare Cropland	Ploughed Agriculture Land	Agriculture
7	Built-up	Settlements	Human Settlement
8	Bare Soil	Exposed Surface	Natural Surfaces

Source: Author's classification adapted from Anderson *et al.* (1976) land cover classification framework for artisanal mining contexts, Du Area

2.4 Spatiotemporal Analysis

Change detection analyses included: (1) 8-class annual area change and magnitude quantification (2010–2015); (2) Mollusce LULC transition matrices examining 8×8 class combinations (2010–2025); (3) Nearest Neighbour Analysis tracking temporal pixel distribution of ASM activity; and (4) Four-Category Severity Classification Framework categorizing transitions as No Change, Degradation, Improvement, or Neutral Transition. Final outputs include Multi-Temporal LULC maps (2010–2025), Transition Matrix & Severity maps, and Nearest Neighbour Analysis visualizations.

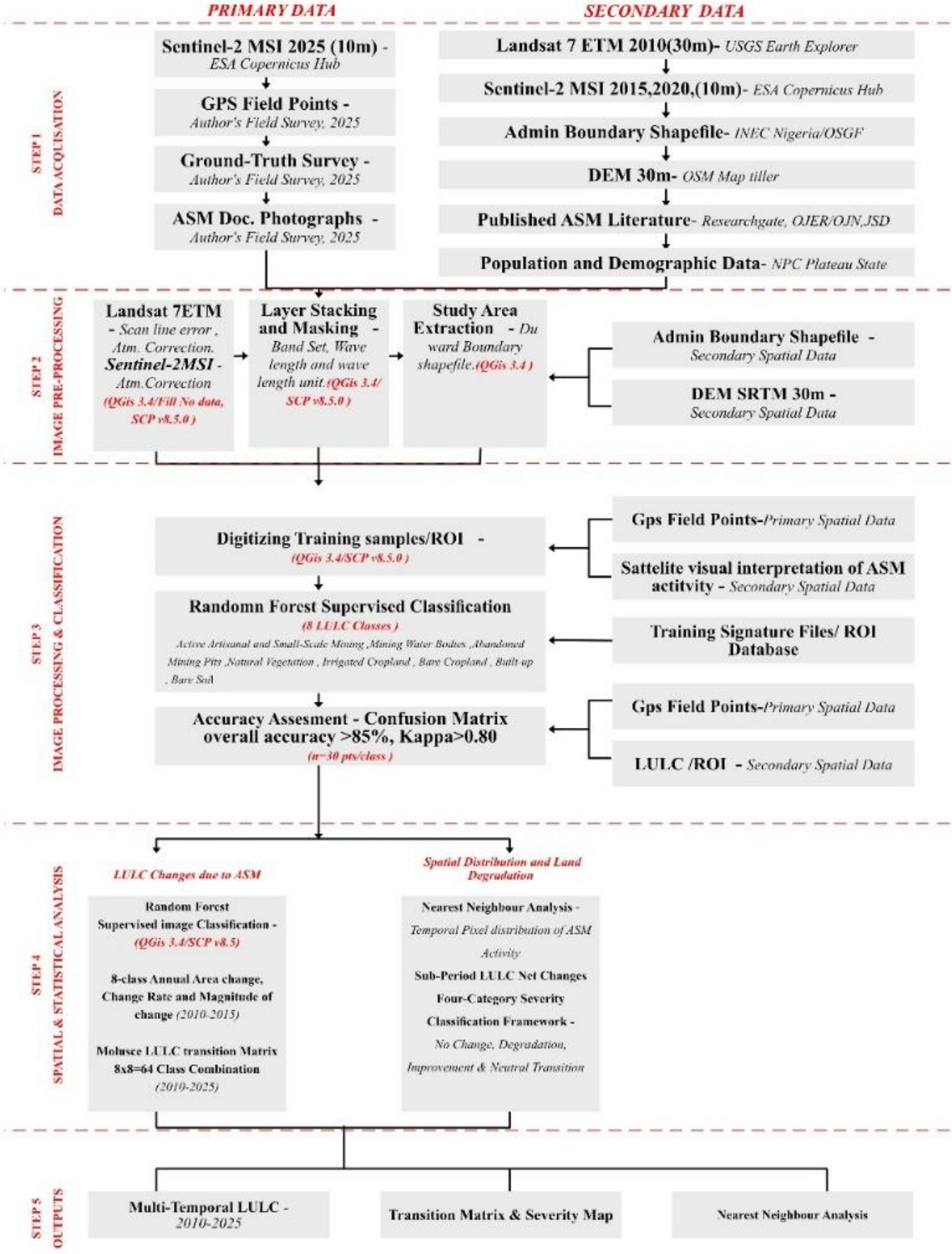

Figure 2: Research Design
Source: Modified from (Fonseca et al., 2024; Gligor et al., 2024; Kumi-Boateng & Stemn, 2020)

2.5 Data Analysis

2.5.1 LULC change detection and transition matrix

LULC change detection was performed using the MOLUSCE plugin in QGIS, cross-tabulating the 2010 and 2025 classified rasters to generate an 8×8 transition matrix (64 class combinations), quantifying the area in hectares and proportional probability of transition between all LULC class combinations. Sub-period net change statistics were derived for the three 5-year intervals (2010–2015, 2015–2020, 2020–2025) to identify the temporal phases of ASM-driven LULC transformation.

2.5.2 Nearest Neighbour Analysis

ASM site centroids were extracted from classified rasters for all four study periods using QGIS raster-to-vector conversion tools. The Nearest Neighbour Index (NNI) was computed for each period using QGIS vector analysis tools: NNI = D_obs / D_exp, where D_obs is the observed mean nearest-neighbour distance and D_exp = 0.5 / √(n/A), with n = point count and A = study area. A z-score was computed to assess statistical significance at the 95% confidence level ($p < 0.05$). NNI < 1.0 indicates clustering; NNI > 1.0 indicates dispersion.

3 Results and Discussions

3.1 LULC Changes due to Artisanal and Small-Scale Mining (ASM) Activities in Du Area (2010–2025)

The Du district has experienced notable changes in mining site distribution between 2010 and 2025 as a result of artisanal and small-scale mining (ASM) activities. These changes were predominantly concentrated within proximity to active mineral extraction sites during the colonial-era mining exploration. Table 1 and Figure 2 present the classification scheme of the eight LULC categories identified throughout the study period, which forms the basis for the analyses conducted in this section.

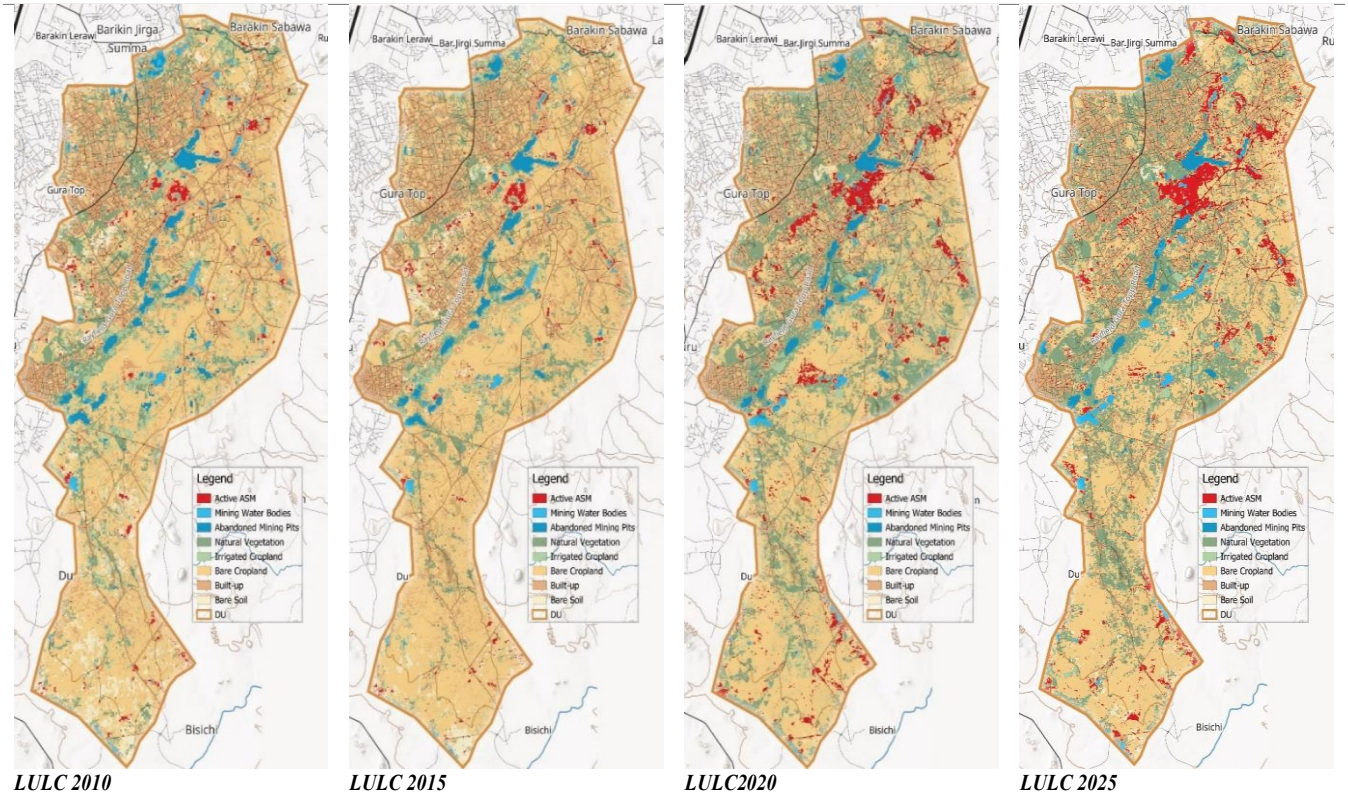

Figure 3: Multi-temporal Land Use / Land Cover Classification Maps of Du: 2010, 2015, 2020, and 2025

The land use and land cover (LULC) change classification statistics for the Du Area across the 15-year study period (2010-2025) as shown in Table 2 using a 5-year interval with three sub-periods: 2010-2015, 2015-2020, and 2020-2025, reveals that the environment is undergoing significant and accelerating change, driven primarily by the spatial expansion and intensification of artisanal and small-scale mining (ASM) activities alongside parallel losses in agricultural land, bare soil, and the built-up area.

The 15-year LULC analysis reveals dramatic landscape transformation in Du, dominated by Active ASM expansion (348% increase, +375 ha at 25% annual rate) and Natural Vegetation recovery (128% increase, +1,038.27 ha), indicating post-mining ecological succession. Conversely, Bare Soil declined steeply (−75.44%), suggesting vegetation colonization of degraded surfaces, while Built-up areas contracted significantly (−28.14%), reflecting rural out-migration. Irrigated Cropland experienced a severe decline (−62.75%), indicating ASM displacement of agricultural livelihoods, though Bare Cropland remained relatively stable (−3.89%), suggesting partial agricultural persistence. Mining Water Bodies and Abandoned Pits showed marginal changes, implying mining site stabilization post-2010. The paradoxical simultaneous increase in both Active ASM and Natural Vegetation suggests spatial heterogeneity—vegetation recovery in areas distant from mining operations, while ASM intensifies in localized hotspots. Overall, these dynamics reflect a landscape undergoing rapid anthropogenic modification through mining intensification coupled with secondary vegetation regrowth on abandoned agricultural and degraded lands, reshaping Du's ecological and socioeconomic profile over the 15-year period.

Table 2: LULC Area and Change Statistics, DU (2010-2025)

LULC Class	2010 (ha)	2015 (ha)	2020 (ha)	2025 (ha)	Δ (ha)	Δ %	Ann. Rate %
Active ASM	107.76	136.18	436.10	482.76	375.00	348.01	25.00
Mining Water Bodies	97.44	64.40	81.33	86.20	-11.24	-11.54	-0.75
Abandoned Pits	171.63	134.11	127.18	125.32	-46.31	-26.98	-3.09
Natural Vegetation	808.65	735.64	1599.71	1846.92	1038.27	128.40	69.22
Irrigated Cropland	521.13	284.55	556.30	194.12	-327.01	-62.75	-21.80
Bare Cropland	3309.23	3902.93	3077.10	3180.48	-128.75	-3.89	-8.58
Built-up	1932.83	1858.83	1469.25	1388.88	-543.95	-28.14	-36.26
Bare Soil	471.93	303.97	73.63	115.92	-356.01	-75.44	-23.73
	7420.60	7420.60	7420.60	7420.60			

Figure 3 reveals the directional probabilities of land cover transition across all 64 class combinations between 2010 and 2025, confirming a landscape dominated by degradation persistence and inadequate recovery. The diagonal persistence probabilities expose structurally entrenched land cover states. Bare cropland exhibited the highest persistence at 58.67%, confirming a stable degraded equilibrium resistant to natural recovery; abandoned mining pits persisted at 46.51%, indicating near-zero passive rehabilitation; and active ASM retained 44.79% of its 2010 extents, confirming continued operational intensity.

The most critical off-diagonal degradation pathway is natural vegetation transitioning to bare cropland (18.37%), representing the largest single mechanism of vegetation loss. Irrigated Cropland demonstrated acute vulnerability, with 46.48% transitioning to Natural Vegetation attributable to agricultural abandonment rather than genuine recovery, and a further 30.72% converting to Bare Cropland, confirming irreversible productive land loss. Built-up land showed a notable 30.15% transition to Bare Cropland and 9.55% directly to Active ASM, providing quantitative evidence of mining encroachment displacing residential areas. On the contrary, post-mining recovery transitions remained negligible. Active ASM converting to Natural Vegetation at only 8.48%, and Abandoned Pits recovering to any vegetated class at under 22%, confirming that passive natural regeneration is insufficient to reverse ASM-induced degradation at the current trajectory.

The land use/land cover (LULC) transition matrix derived from the multi-temporal satellite classification cross-tabulates 64 combinations across all eight LULC classes as presented in Table 3, including Active Artisanal and Small-Scale Mining (ASM), Mining Water Bodies, Abandoned Mining Pits, Natural Vegetation, Irrigated Cropland, Bare Cropland, Built-up, and Bare Soil. To interpret the environmental direction and extent of change within the transitions, each combination was assigned to one of four severity categories: No Change, Degradation, Improvement, or Neutral Transition.

Table 3: Summary of LULC Transitions by Severity Category

Severity Category	No. of Transitions	% of Count	Total Area (ha)	% of Study Area
No Change	9	14.1%	3,277.80	44.2%
Degradation	37	57.8%	3,020.04	40.7%
Improvement	12	18.75%	581.48	7.9%
Neutral Transition	6	9.38%	541.28	7.3%
TOTAL	**64**	**100%**	**7,420.60**	**100%**

3.2 Spatial Distribution of ASM Sites in Du

A total of 86 GPS points were recorded across 23 localities within the Du Area study during field observation, as illustrated in Figure 5a. The spatial distribution of mining sites reveals a random pattern cluster that matches the zones of ASM activity identified in the 2025 Sentinel-2 LULC classification. With the Kwang axis, surrounding Dura (n=6); Loyep Kwang (n=6); Vwuzi Kwang (n=6); Kwang Hei (n=3); Lojang Estate Kwang (n=1); and Zot Rak Kwang (n=1), collectively accounting for 23 points (26.7% of total). Other sites are the central Du corridor, comprising Dwei (n=8), Topp Rayfield (n=6), Latya (n=3), Jerek (n=3), Little Rayfield (n=4), and Gura Topp Rayfield (n=1), with 25 points (29.1%). The central-western and Du Village axis encompassing Du Village (n=2), Fwati Du (n=2), Dyenkai Koroshi Du (n=2), Ladura Du (n=3), and Bwi-logwom (n=3) accounts for 12 points (14.0%). The southern region, Karinji Stream (n=6), Kung Bwuna Du (n=6), and Ratyi Du (n=6), records 18 points (20.9%). The 8 points (9.3%) at Doi (n=7) and Lekwu Du Kwang (n=1) occupy the eastern margin of the study area (also see Figure 3).

While the temporal expansion of artisanal and small-scale mining activity revealed that active ASM was the least land cover class in 2010, covering 108.64 ha of Du. Between 2010 and 2015, mining activity grew slowly, adding only 27.72 ha to the spread, 136.36 ha, a minimal increase of 25.5% that reflected the early, low-intensity character of artisanal mining during this phase. The period between 2015 and 2020 witnessed the peak of artisanal and small-scale mining activity and the most significant expansion in the entire study period, with active mining land nearly tripling from 136.36 ha to 437.12 ha, a gain of 300.76 ha (+220.6%) within the duration of five years. This rapid growth marked the most damaging and environmentally impactful phase of ASM activity recorded across the full observation period. Between 2020 and 2025, the rate of expansion slowed considerably but continued to rise, with active mining land reaching 482.76 ha, its greatest recorded extent across all four study years.

Overall, active mining land grew by 374.08 ha (+346.5%) over the 15 years at an average annual rate of 10.49%, confirming that ASM expanded continuously, significantly, and without interruption throughout the Du Area study period. (see Figure 4b).

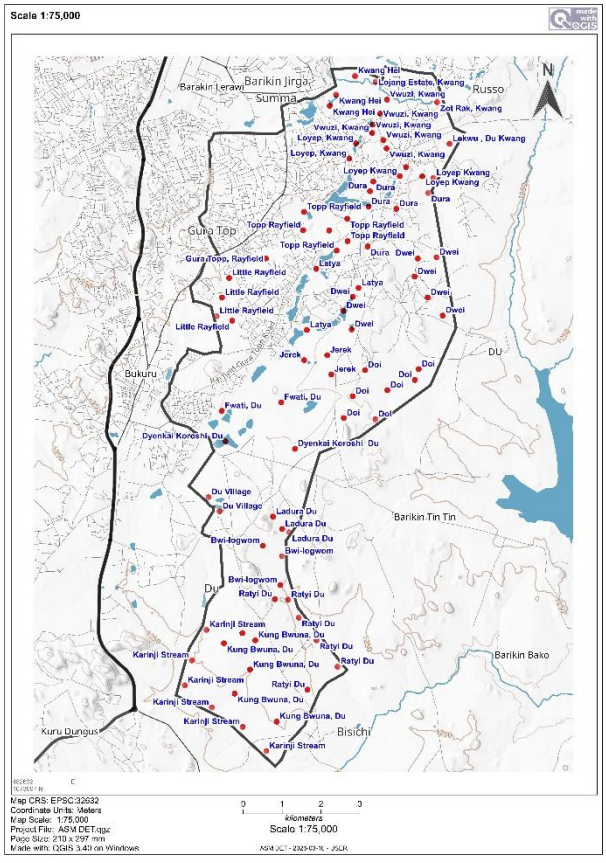

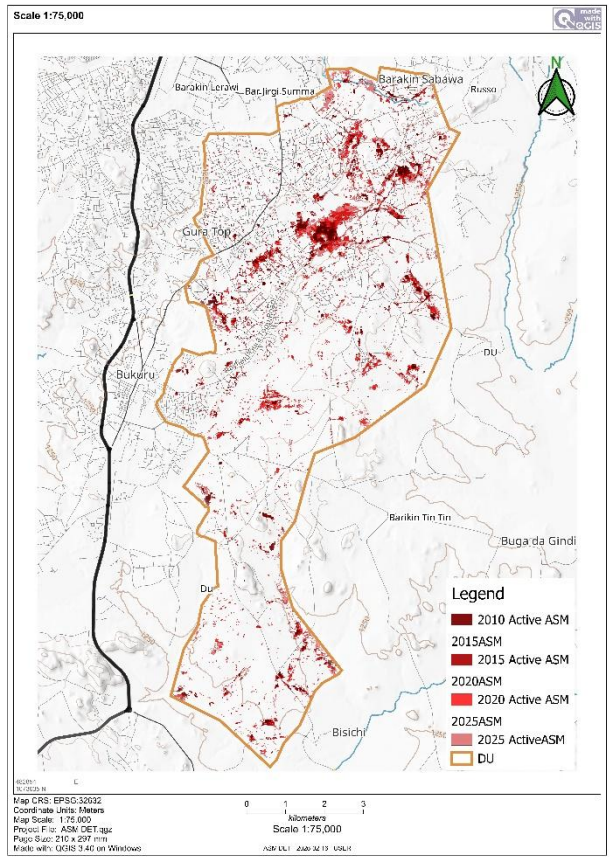

Figure 4: a) Spatial Distribution of ASM Activities in Du. *b) Temporary Changes of ASM Activity in Du*

Furthermore, a nearest neighbour analysis was conducted across all four classification periods to further justify the spatial distribution pattern of ASM activity in the Du Area between 2010 and 2025 results consistently revealed the nearest neighbour index values below 1.0 and z-scores far exceeding the −1.96 significance threshold across all periods (2010: R = 0.526, z = −30.08; 2015: R = 0.544, z = −29.82; 2020: R = 0.643, z = −33.86; 2025: R = 0.652, z = −34.20; all $p < 0.001$). Table 4 presents the Nearest Neighbour Analysis ASM Centroid Results (2010–2025). Results in 2010 with a Nearest Neighbour Index of 0.5255 (z = -30.08) record one of the most intense clusterings of the ASM site. With an observed mean distance of only 92.06 m, contrary to an expected random distance of 175.18 m, ASM sites in 2010 were concentrated within an existing mineral extraction zone, reflecting the legacy concentration of artisanal activity around former colonial-era tin and columbite workings. The z-score of −30.08 ($p < 0.001$) confirms this is highly statistically significant. While in 2015, the Nearest Neighbour Index was 0.5439 (z = -29.82), the 2015 pattern remains strongly clustered, with a slightly higher index (0.5439) than in 2010, indicating a very slight dispersal tendency of new ASM sites added. However, clustering remains extreme, and the near-identical observed mean distances (92.06 m and 92.28 m) confirm that new sites opened near existing. The highest shift in the entire dataset occurs between 2015 and 2020, with 2020 NNI recorded (z = −33.86, rising from 0.5439 to 0.6429), confirming that ASM expansion occurred during this period. This confirms directly with the +300.84 ha (+220.7%) active ASM area expansion recorded in the LULC analysis between 2015 and 2020. The 2025 results show continued clustering with a slightly higher index of 0.6519(z = −34.20) over the smallest observed mean distance of all four study periods (72.22 m). This marginal NNI increase does not indicate dispersal; it reflects a maturing and stabilizing cluster structure as ASM activity within recognized degradation hotspots.

Table 4: Nearest Neighbour Analysis of ASM Raster Pixel Count (2010–2025)

Year	Obs. MD (m)	Exp. MD (m)	NNI (R)	Pixel Count	Z-Score	Sig.	Pattern
2010	92.06	175.18	0.5255	1,098	−30.08	$p < 0.001$	Strong Clustering
2015	92.28	169.66	0.5439	1,168	−29.82	$p < 0.001$	Strong Clustering
2020	73.20	113.85	0.6429	2,457	−33.86	$p < 0.001$	Strong Clustering
2025	72.22	110.77	0.6519	2,638	−34.20	$p < 0.001$	Strong Clustering

The 2015–2020 interval produced the most significant shift in all NNA metrics: the NNI increased by +0.099 (the largest single-period change), 1,289 new sites were added (+110.4%), and the mean inter-site distance decreased by 19.08 m. This pattern of intensifying clustering concurrent with explosive site proliferation is consistent with the 'infilling' dynamic documented by Couttenier et al. (2022), in which new ASM workings open within the footprint of established clusters rather than expanding into new geographic zones. By 2025, NNI = 0.6519 (z = −34.20) with the smallest observed mean distance of all four periods (72.22 m), confirming that ASM activity has reached a mature, tightly packed cluster structure within recognized degradation hotspots. The null hypothesis of random ASM distribution is conclusively rejected across all four time periods.

4 Limitation

A critical constraint is sensor mismatch and scan line error: Landsat 7 ETM (2010) provides 30m multispectral resolution, while Sentinel-2 MSI (2015, 2020, 2025) offers 10m resolution. This resolution difference has an influence on temporal consistency and increases potential classification errors in smaller ASM patches (<30m). Landsat 7's SLC-off malfunction (2003) required gap-filling during preprocessing. Differing spectral band configurations between sensors required radiometric normalization, image masking, and LULC transitions. Cloud cover limitations further constrained available imagery for optimal seasonal analysis. These constraints may affect change magnitude estimates and small-scale mining feature detection accuracy across the 15-year timeline.

5 Conclusion

The study revealed that artisanal and small-scale mining (ASM) in Du Area, Jos South, has led to rapid and spatiotemporal concentrated land use/land cover changes and exhibits a pronounced spatial distribution pattern between 2010 and 2025. It further demonstrated that Active ASM activities expanded greatly by resulting in widespread landscape transformation. This is characterized by a dominance of degradation over recovery. Spatial analysis confirmed that ASM activities are strongly clustered across all study periods. Nearest Neighbourhood Analysis confirms statistically significant clustering, indicating that mining activities are concentrated within hotspot zones that can be identified.

The observed increase in clustering intensity reflects progressive spatial saturation, where new mining sites develop in proximity to existing ones rather than dispersing into new areas. It should be noted that ASM-induced changes are not random but spatially structured, requiring targeted and data-driven management approaches for effective environmental restoration and sustainable land use planning.

As observed from the study, it is relevant to recommend that a standardized satellite-based LULC Monitoring and reporting Framework be established by Government agencies to track land use changes at regular intervals (e.g., every five years) and support evidence-based environmental regulation. A centralized geospatial database of multi-temporal LULC data should also be developed and maintained to serve as a baseline for continuous environmental monitoring, planning, and decision-making in the Du Area.

Based on the identified clustering patterns of ASM activities, spatial control or exclusion zones around sensitive areas such as farmlands, water bodies, and settlements should be delineated and enforced to prevent further environmental encroachment. A real-time GIS-based monitoring system should be introduced to track the location and expansion of ASM sites, enabling early detection of new mining activities and improving regulatory control.

References

Adeyemi, O., & Olagunju, T. (2015). Risk perception in a southwestern mining community in Nigeria. Journal of Environmental Management and Safety, 6(1), 1–12.

Anderson, J. R., Hardy, E. E., Roach, J. T., & Witmer, R. E. (1976). A land use and land cover classification system for use with remote sensor data (USGS Professional Paper 964). United States Geological Survey

Bala, A., Garba, S., & Adewuyi, T. (2021). Geospatial analyses of mining-induced land degradation sites in Jos South Local Government Area, Plateau State, Nigeria. Researchgate. https://www.researchgate.net/publication/352771455

Congedo, L. (2021). Semi-Automatic Classification Plugin: A Python tool for the download and processing of remote sensing images in QGIS. Journal of Open-Source Software, 6(64), 3172. https://doi.org/10.21105/joss.03172

Couttenier, M., Rollo, S. Di, Inguere, L., Mohand, M., & Schmidt, L. (2022). Mapping artisanal and small-scale mines at a large scale from space with deep learning. PLoS ONE, 17(9).

https://doi.org/10.1371/journal.pone.0267963

Fonseca, A., Marshall, M. T., & Salama, S. (2024). Enhanced detection of artisanal small-scale mining with spectral and textural segmentation of Landsat time series. Remote Sensing, 16(10). https://doi.org/10.3390/rs16101749

Gligor, V., Nicula, E. A., & Cretan, R. (2024). The identification, spatial distribution, and reconstruction mode of abandoned mining areas. Land, 13(7). https://doi.org/10.3390/land13071107

Gospel, C., Rachael, C., Ulunma, O., Christian, C., Ogechi, C., Uzoamaka, F., & Gabriel, C. (2020). Assessment of trace metals contamination on soil from abandoned artisanal tin mining paddock in Barkin-Ladi Area of Plateau State. International Journal of Advanced Academic Research, 11. https://doi.org/10.46654/ij.24889849

Kumi-Boateng, B., & Stemn, E. (2020). Spatial analysis of artisanal and small-scale mining in the Tarkwa-Nsuaem Municipality of Ghana. Ghana Mining Journal, 20(1), 66–74. https://doi.org/10.4314/gm.v20i1.8

Mafuyai, G. M., Ayuba, & Zang, C. U. (2020). Physico-chemical characteristics of tin mining pond water used for irrigation in Plateau State, Central Nigeria. Open Journals Nigeria. www.openjournalsnigeria.org.ng

Merem, E. C., Twumasi, Y., Wesley, J., Isokpehi, P., Shenge, M., Fageir, S., Crisler, M., Romorno, C., Hines, A., Hirse, G., Ochai, S., Leggett, S., & Nwagboso, E. (2017). Assessing the ecological effects of mining in West Africa: The case of Nigeria. International Journal of Mining Engineering and Mineral Processing, 6(1), 1–19. https://doi.org/10.5923/j.mining.20170601.01

Muromba, T. G., & Xu, L. (2024). A GIS and remote sensing approach in assessing impacts of mining in Chegutu District, Zimbabwe. OALib, 11(12), 1–31. https://doi.org/10.4236/oalib.1112635

Nava, L., Cuevas, M., Meena, S. R., Catani, F., & Monserrat, O. (2022). Artisanal and small-scale mine detection in semi-desert areas by an improved U-Net. IEEE Geoscience and Remote Sensing Letters, 19. https://doi.org/10.1109/LGRS.2022.3220487

Ndace, J. S., & Danladi, M. H. (2012). Impacts of derived tin mining activities on land use/land cover in Bukuru, Plateau State, Nigeria. Journal of Sustainable Development, 5(5). https://doi.org/10.5539/jsd.v5n5p90

Nigerian Meteorological Agency (NIMET). (2023). Annual Climate Review Report. NIMET, Abuja, Nigeria.

NPC. (2024). Du Ward population estimate. NPC Plateau State Office, Ref. No. NPC/PL/CEN/24/VOL.I/72.